

Controlling transistor threshold voltages using molecular dipoles

Smitha Vasudevan,¹ Neeti Kapur,² Tao He,^{3,4} Matthew Neurock,^{2,5} James M. Tour,^{3,6} and Avik W. Ghosh¹

¹Department of Electrical and Computer Engineering,
University of Virginia, Charlottesville, VA 22904

²Department of Chemical Engineering, University of Virginia, Charlottesville, VA 22904

³Department of Chemistry, Rice University, Houston, TX 77005

⁴Smalley Institute for Nanoscale Science and Technology, Rice University, Houston, TX 77005

⁵Department of Chemistry, University of Virginia, Charlottesville, VA 22904

⁶Smalley Institute for Nanoscale Science and Technology, Rice University, Houston, TX 77005

We develop a theoretical model for how organic molecules can control the electronic and transport properties of an underlying transistor channel to whose surface they are chemically bonded. The influence arises from a combination of long-ranged dipolar electrostatics due to the molecular headgroups, as well as short-ranged charge transfer and interfacial dipole driven by equilibrium band-alignment between the molecular backbone and the reconstructed semiconductor surface atoms.

Inorganic semiconductors have traditionally dominated as the material players in the electronics industry. While their organic counterparts have been studied extensively as alternate channel materials [1], the development of a stand-alone molecular electronics technology has been stymied by the inordinate difficulty of contacting small molecules reproducibly, their insufficient mobilities, large RC constants and poor gateability. Perhaps a more promising approach is to envisage hybrid organo-semiconductor devices, combining the established infrastructure of the semiconductor integrated industry with the ‘bottom-up’ self-assembly and chemical tunability of molecular monolayers. A particularly interesting possibility is to use organic molecules to control the surface properties of deeply scaled, backgated silicon transistors, by tying up deleterious surface states and charge transfer ‘doping’. In addition, monitoring the transistor dynamics, such as the shift in its threshold voltage, can be used to detect a single molecule adsorption event [2]. It is thus critical to properly understand the physical factors that determine how a molecule controls a transistor, and how the transistor, in turn, senses the molecule.

In this paper, we develop a quantitative theory for the threshold voltage control of low-doped silicon channels by surface bonded organic monolayers with varying dipole moments. We focus in particular on a recent series of experiments [4] that involved the grafting of molecular monolayers atop oxide free H-passivated silicon surfaces. The choice of the molecules followed an important logic. An identical set of molecules was used, with the exception of one substituent group. This allowed a systematic study of the effect of the molecules on the electrical properties of the device. While organic molecules attached to semiconductor surfaces have been studied extensively [5, 6, 7], albeit phenomenologically, our principal challenge is to develop a quantitative, ‘first principles’ model that combines atomistic charge-transfer processes with macroscale electrostatics. We employ Density Functional Theory (DFT) to extract the molecular adsorption geometry, interfacial dipole and band-alignment at the atom-

istically reconstructed silicon surface. These quantities are then incorporated as inputs into a macroscopic Poisson solver to compute the band-bending in the transistor channel. The calculated threshold voltage shifts and band-alignments are in excellent agreement with experiments for multiple molecules (Table I) [4].

Given the low doping and likely statistical fluctuations in data, as well as uncertainties in the experiment (for instance, in the number of bonded molecules), there is undoubtedly some wiggle room for theory that may make this correspondence fortuitous. However, the main trend in the experiment seems quite robust, namely, a clear monotonic dependence of the threshold voltage on the dipole moment of the headgroup. This is borne out quite well by our model. In addition, we demonstrate the accuracy of our model by comparing our computed intermediate ingredients with complementary experimental data obtained on the same set of samples [8].

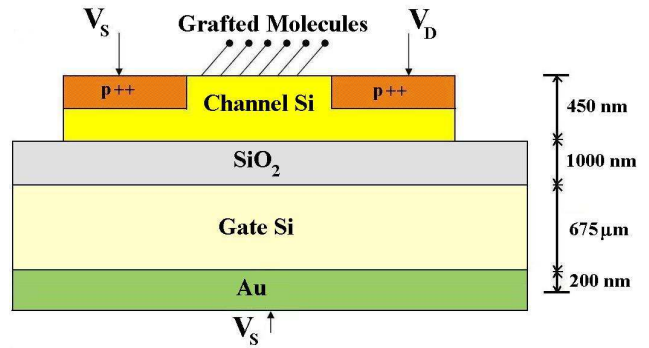


FIG. 1: Schematic side-view representation (not to scale) of the pseudo-MOSFET under investigation [4]. The molecules were grafted between the source and drain electrodes. V_S , V_D , and V_G refer to the bias applied on the source, drain, and gate, respectively.

Molecule free device. The devices we are studying were fabricated using a silicon-on insulator (SOI) wafer [4]. A back gated structure was used to allow easy grafting of a molecular monolayer on the silicon device top layer

(Fig.1). The molecules were grafted on H-passivated silicon surfaces using diazonium based chemistry (molecules lose the diazonium group to form radicals before attaching to the surface[9]). In the fabricated MOSFET, the bulk p-Si substrate (handle) was biased at V_G using the gold back contact and acts as a gate terminal. This in turn induces a conduction channel at the upper interface of the buried oxide, used as a gate dielectric layer. The conducting channel corresponds to the formation of an accumulation layer (p-channel). In practice, the drain current voltage characteristic presents a linear behavior at low drain voltages V_D , and tends to saturate as the drain voltage approaches the voltage difference between the gate bias and the threshold voltage. In the diffusive transport regime, the current-voltage characteristics are satisfactorily described by the square law theory [10](Fig.2)

$$I = \frac{qC_G\mu W}{2L} \left[V_G - V_T - \frac{V_D}{2} \right] V_D \quad (1)$$

where W and L are the channel width and length, C_G is the gate capacitance and μ is the channel mobility. In this case, an accumulation channel is activated when both the gate and the drain are negatively biased. Because the transistor body is the nearly intrinsic p-Si layer, the channel is assumed to be completely accumulated.

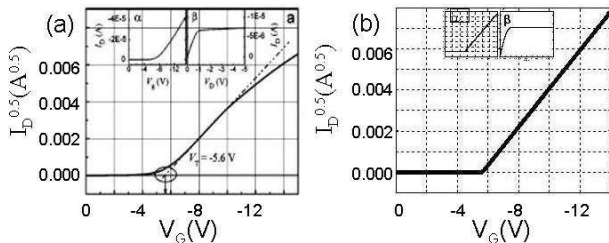


FIG. 2: (a) Experimentally obtained I-V characteristics [4] of the fabricated MOSFET devices. Inset (α) displays the typical transfer characteristics of the devices under test. Inset (β) shows the typical output characteristics of the devices under test. (b) Theoretically calculated I-V characteristics of the MOSFET device.

An accumulation mode transistor is not expected to have a prominent turn-on as one expects for an inversion channel transistor. The onset voltage is associated with pulling the contact Fermi energies below the valence band-edge near the oxide interface. The large threshold voltage values of the bare MOSFET ($\sim -5.6V$) could be indicative of traps at the oxide-channel interface. This is further confirmed by the presence of prominent hysteretic signatures that suggest charge trapping processes. We used two approaches to estimate the areal density of interfacial traps in the control devices. The first assumes that the threshold voltage of the control devices is due to trapped charge on one side of a capacitor, with a capacitance/area equal to C_{ox} . Using this

method, the density of interfacial traps was calculated to be $N_i = Q_F/q = |\Delta V_T| \times C_G/q = 1.2 \times 10^{11}/cm^2$. The second approach estimates the same quantity using the observed subthreshold swing S [11]. The traps would degrade the subthreshold current by taking away some of the mobile charges that would otherwise have contributed to current flow. The interfacial trap density is calculated to be $N_i = SC_G \log_{10} e/(kT/q) = 1.0 \times 10^{11}/cm^2$. The consistency of the two estimates strengthens our arguments as to the origin of the threshold voltage and subthreshold slopes observed.

Molecular attachment. Quantum-chemical calculations were carried out using DFT as implemented in the Vienna Ab-initio Simulation Package (VASP) [12, 13]. Plane wave basis sets were used to represent the atoms and the PW91 form of the GGA functional was used to carry out gradient corrected calculations. The optimized structures for the isolated gas-phase molecules under consideration, dimethylaminobenzene, aniline and nitrobenzene and the corresponding radical forms are shown in Fig.3. These structures were obtained using spin-polarized calculations, and are in agreement with published experiments and theoretical computations [14, 15].

The Si(100) slab was modeled using 9 atomic layers and hydrogen atoms were attached on the lowest layer of the slab to passivate the dangling bonds on the lower slab surface. Geometry optimizations were carried out while constraining the lowest 4 layers of the Si(100) slab at their bulk positions including the hydrogen atoms attached on the lowest atomic layer. We started with a dimerized Si(100) structure as our initial guess (with broken symmetry), and recovered the expected 2x1 reconstructed structure. The dipole moments and vibrational modes were calculated within VASP using single point calculations.

Once our isolated geometries were thoroughly benchmarked, we moved on to the adsorption geometry. The radical forms of the molecules we studied, specifically, dimethylaminobenzene, aniline and nitrobenzene, were adsorbed on the asymmetrically dimerized Si(100) slab via a C-Si covalent bond. We considered two possible adsorption sites on the Si(100) slab, named T1 and T2. In all the cases considered for atop adsorption of radicals on the surface, we find that the radicals stand normal to the surface. A positive dipole, with the positive pole directed toward the semiconductor surface, is induced by nitrobenzene, while a negative dipole is induced by aniline and dimethylaminobenzene. Table I shows the computed dipole moments.

Threshold Voltage Shift. The presence of the molecular layer modifies the silicon surface work function, which in turn affects the device properties. The work function (WF) is the minimum energy required for an electron to escape into vacuum from the Fermi level (E_F) of the material, and is determined by (i) the electron affinity (EA), the energy required to excite an electron from the bottom

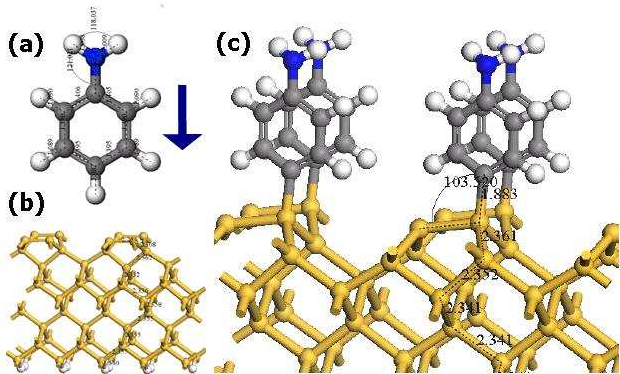


FIG. 3: Optimized geometries for the (a) gas-phase molecule aniline (arrow points in the direction of dipole moment, from positive to negative charge). (b) Optimized structure for passivated Si(100) slab with symmetrically dimerized surface. (c) Optimized structure for aniline radical adsorbed on passivated Si(100)-(2x1) slab atop site T1 (top atom of the dimer).

of the conduction band (CB) at the surface to the local vacuum level; (ii) the band bending (BB), the electrical potential difference between the surface and the electrically neutral semiconductor bulk; and (iii) the energy difference between the bulk CB and the Fermi level. ΔWF can be due to ΔEA , ΔBB , or both. We computed the total shift directly from the shift in the estimated highest occupied molecular orbital (HOMO) level of the molecule before and after adsorption. This was accomplished by comparing the projected density of states on the silicon atoms, which is maximized for the HOMO levels of benzene-based molecules [16]. The computed shifts agree

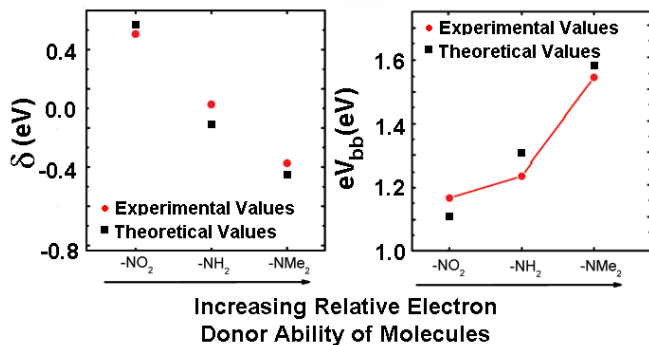


FIG. 4: Comparison of calculated values and experimental UPS/IPES/XPS data. Experimental data are adapted from [8]

very well with experimental data, as seen from the last two columns of Table I, as well as comparisons with ultraviolet photoelectron spectroscopy (UPS) and inverse photoemission spectroscopy (IPES) data combined with X-ray photoelectron spectroscopy (XPS) data (Fig. 4). The shift shows a monotonic dependence on the dipole mo-

ment of the headgroup, which is quite encouraging. Surprisingly, however, there is an additional shift relative to the H-passivated control, which is unexpected (thus, the threshold voltage shifts of the nitro and amino components do not straddle that of the control, but lie on the same side of it). We will now attempt to deconstruct the computed shifts to understand their physical origins. *Dipolar Contribution.* The electron affinity of a given surface is directly affected by a surface dipole, which creates an electrical potential drop across the grafted molecular film depending on the dipole moment. Simply put, a positive headgroup such as NH_2 acts as a gate that pulls negative charges to the surface, lowering its local electronic levels, while NO_2 pushes them away (Fig. 5). The resulting band-bending at the surface propagates towards the opposite end where the oxide sits, penetrating up to a Debye length $L_D = \sqrt{\epsilon_r \epsilon_0 k_B T / N_A q^2}$, where ϵ_r is the dielectric constant of the channel, ϵ_0 is the permittivity of free space, T is the temperature and N_A is the acceptor dopant density.

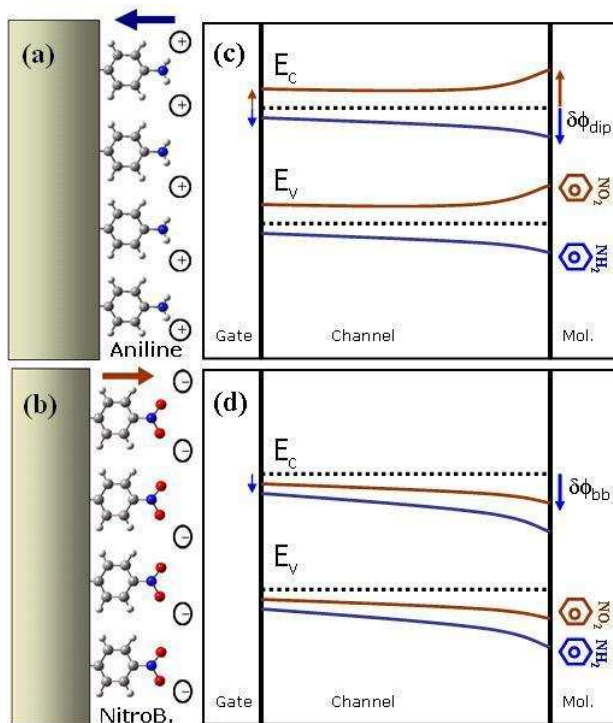


FIG. 5: Adsorbed layer of (a) Aniline (Blue line) and (b) Nitrobenzene (Brown line) molecules, creating dipole moments on the surface. (c) Energy Band Diagram for the system being studied. (d) Pictorial representation of change in band bending due to charge transfer between molecular monolayer and substrate.

The purely dipolar headgroup gives a shift in potential given by

$$\delta\phi_{dip} = (N_{mol} \mu_{dip} \cos\theta / \epsilon_m) e^{-t_{si}/L_D} \quad (2)$$

where N_{mol} gives the areal surface density of the attached

TABLE I: Data of computed dipoles of the molecule-semiconductor system, shifts due to dipole (ϕ_{dip}) and charge transfer (ϕ_{bb}), computed and experimental changes [4] in the threshold voltage of the devices. The control consists of an H-passivated Si(100) surface.

Systems	μ_{dip}	$\delta\phi_{dip}$	$\delta\phi_{bb}$	$\Delta V_T(V)$	$\Delta V_T(V)$
	(dB)	(V)	(V)	Theory	Expt.
Control	0.03	0.0058	0	0.0058	0
Nitro	2.17	0.22	-0.725	-0.525	-0.55
Aniline	-1.44	-0.14	-0.96	-1.1	-1.25
Dimethylaminobenzene	-1.65	-0.28	-1.12	-1.4	-1.55

molecules, μ_{dip} is the static dipole moment of each molecular head group oriented at an average angle θ relative to the normal to the surface, ϵ_m is the molecular dielectric constant, and t_{si} is the thickness of the channel silicon. This contribution is opposite for opposite dipolar signs. Significantly, dipolar gating at the top surface nontrivially influences the threshold voltage at the backgate owing to the large Debye length associated with low doping in the channel. For a doping level of $10^{13}cm^{-3}$ the Debye length $L_D \sim 1.25\mu m$, so that the exponential transfer factor is around 0.7 (implying that seventy per cent of band-bendings at the surface are transmitted to the bottom end).

Charge-Transfer Barrier. In addition to the dipolar contribution, the molecular monolayers also transfer spectral weight to the semiconductor surface through bonding. Because the mobile charges are primarily near the bottom of the channel, this does not add significant additional resistance, but it does influence the local band-bending through the charge-transfer dipole at the molecule-semiconductor interface. Based on our computed shifts and the dipolar contributions separately extracted, we can compute this component for each molecule. To zeroth order, this represents the charge transfer due to the workfunction difference between the headgroup-free molecular backbone (the bare benzene ring) and the silicon surface. This means that the associated band-bending is in the same direction for all the headgroups (Fig.5b), and relatively weakly varying with dipole moment (column 4 of Table I). There is, however, some variation, indicating that the separation into a purely dipolar part and a head-group independent backbone part is not strictly feasible, owing to the short length of the benzene rings and the resulting hybridization between the ring states and the headgroups. The electron donating ring electrons push charge towards the p-Si substrates and become partly positively charged, leading to an increase in the positive surface charge density and a lowering of the local silicon surface levels (Fig.5b). The donating capacity, however, is enhanced (diminished) by the electronegativity (positivity) of the headgroups. Methylamine has the highest electron-donation capability, and hence provides the highest change in charge-transfer induced band bending $\delta\phi_{bb}$. While we do not independently compute $\delta\phi_{bb}$, one

can roughly estimate this by calculating the charge neutrality level E_{CNL} of the headgroup molecular backbone (CNL is defined as the energy to which electrons need to fill the molecule to keep it electrically neutral – frequently this is replaced by the LUMO level [7]). The work-function shift of the molecule is then given by

$$\delta\phi_{bb} \approx \frac{(E_F - E_{CNL})e^{-t_{ch}/L_D}}{1 + 1/U_0D_0} \quad (3)$$

where U_0 is the single-electron charging energy of the molecule and D_0 is its density of states near the Fermi energy. The barrier height $E_F - E_{CNL}$ is of the order of 1 V for aromatic molecules on silicon [7], giving us the correct observed order of magnitude. The term in the denominator includes the Coulomb cost for charging up the molecule. In this contribution, we have studied the effects, both qualitatively and quantitatively, of grafting molecular monolayers on the top surface of backgated MOSFETS. Such a scheme of using molecules on surfaces to tailor device properties is becoming increasingly attractive as devices get smaller, and surface-to-volume ratios increase vastly. The study of surface modifications could also have practical implications for sensors, specifically chemically sensitive field-effect transistors (CHEMFETs)[17]. A radically different principle of operation that we are working on [18] involves a stronger bonding between the molecule and the channel, involving actual wavefunction overlap, leading to quantum scattering by the molecular traps that creates characteristic fingerprints when scanned with a back gate.

We would like to acknowledge discussions with Tao He, Jim Tour, Lloyd Harriott, John Bean, Neil Di Spigna, Paul Franzon, Pradeep Nair and Ashraf Alam. This work was supported by the NSF-NIRT and NSF-CAREER awards under grants GA10646-128609 and GA10696-129495 respectively.

-
- [1] Reed, M. A.; Lee, T.; Molecular Nanoelectronics; American Scientific Publishers: Stevenson Ranch (2003).
 - [2] Patolsky, F.; Zheng, G.; Lieber, C. M.; *Analyt. Chem.*, vol. **78**, 4260-4269 (2006).
 - [3] Joachim, C.; Gimzewski, J. K.; Aviram, A.; *Nature*, **408** (2000).

- [4] He, T.; He, J.; Lu, M.; Chen, B.; Pang, H.; Reus, W. F.; Nolte, W. M.; Nackashi, D. P.; Franzon, P.D.; Tour, J. M.; J. Am. Chem. Soc., **128**, 14537-14541, (2006).
- [5] Bocharov, S.; Dmitrenko, O.; De Leo, L. P. M.; Teplyakov, A. V; J. Am. Chem. Soc., **128**, 9300-9301 (2006).
- [6] Boulas, C.; Davidovits, J.V.; Rondelez, F.; Vuillaume, D.; Phys. Rev. Lett. ,**76**, 4797-4800 (1996).
- [7] Cahen, D; Naaman, R.; Vager, Z.; Adv. Funct. Mater., **15**, 1571-1578 (2005).
- [8] He, T.; Ding, H.; Peor, N.; Lu, M.; Corley, D. A.; Chen, B.; Ofir, Y.; Gao, Y.; Yitzchaik, S.; Tour, J. M.; J. Am. Chem. Soc., **130**, 1699-1710, (2008).
- [9] Stewart, M. P.; Maya, F.; Kosynkin, D. V.; Dirk, S. M; Stapleton, J. J.; McGuinness, C. L.; Allara, D. L.; Tour, J. M.; J. Am. Chem. Soc., **126**, 370-378 (2004).
- [10] Sze, S. M.; Physics of Semiconductor Devices, Wiley, New York (1981).
- [11] Rolland, A.; Richard, J.; Kleider, J. P.; Mencaraglia, D.; J. Electrochem. Soc. **140**, 3679 (1993).
- [12] Kresse, G.; Furthmuller, J.; Phys. Rev. B,**54**, 11169-11186 (1996).
- [13] Kresse, G.; Furthmuller, J.; Comput. Mater. Sci., **6**, 15-50 (1996).
- [14] Tzeng, W. B.; Narayanan, K.; Shieh, K. C.; Tung, C. C; J. Mol. Struc., **428**, 231-240 (1998).
- [15] Palafox, M. A.; Nunez, J. L.; Gil, M.; J. Mol. Struc., **593**, 101-131 (2002).
- [16] Damle, P. S.; Ghosh, A. W.; Datta, S.; Chem. Phys. **281**, 171 (2002).
- [17] Nikolaidis, M. G.; Rauschenbach, S.; Bausch, A. R.; J. Appl. Phys. **95**, 3811-3815 (2004).
- [18] Vasudevan, S.; Walcak, K.; Ghosh, A. W.; IEEE Sensors Journal, **8**, 857-862 (2008).